

Materials Horizons

Accepted Manuscript



This is an *Accepted Manuscript*, which has been through the Royal Society of Chemistry peer review process and has been accepted for publication.

Accepted Manuscripts are published online shortly after acceptance, before technical editing, formatting and proof reading. Using this free service, authors can make their results available to the community, in citable form, before we publish the edited article. We will replace this *Accepted Manuscript* with the edited and formatted *Advance Article* as soon as it is available.

You can find more information about *Accepted Manuscripts* in the [Information for Authors](#).

Please note that technical editing may introduce minor changes to the text and/or graphics, which may alter content. The journal's standard [Terms & Conditions](#) and the [Ethical guidelines](#) still apply. In no event shall the Royal Society of Chemistry be held responsible for any errors or omissions in this *Accepted Manuscript* or any consequences arising from the use of any information it contains.

Conceptual Insight Statement

A polycrystalline layer of piezoresistive (BEDT-TTF)₂I₃-based molecular conductor is transferred from the parent polycarbonate/(BEDT-TTF)₂I₃ bilayers to silk and other substrates with various shapes and compositions. The transferred layer is robust as confirmed by SEM, temperature dependent resistance, and electromechanical measurements. The silk/(BEDT-TTF)₂I₃ bilayer films are sensitive to moisture, allowing their use for humidity sensing, electrical current driven actuators, and the study of complex moisture diffusion processes.

COMMUNICATION

Silk/Molecular Conductor Bilayer Thin-Films: Properties and Sensing Functions

Cite this: DOI: 10.1039/x0xx00000x

Eden Steven,^{*a} Victor Lebedev,^b Elena Laukhina,^{*b,c} Concepció Rovira,^{b,c} Vladimir Laukhin,^{b,c,d} James S. Brooks,^a and Jaume Veciana,^{b,c}

Received 00th January 2012,
Accepted 00th January 2012

DOI: 10.1039/x0xx00000x

www.rsc.org/

Since their discovery, organic conductors have attracted fundamental and device physics interest due to their diverse physical properties. However, conventional electrochemical growth methods produce millimeter-sized crystals that do not translate to the fabrication of large-scale thin-film devices. Of late a chemical-vapor annealing method has proved capable of growing a conductive polycrystalline layer of (BEDT-TTF)₂I₃ molecular conductor on the surface of soluble polycarbonate (PC) thin films in a bilayer configuration. (Here BEDT-TTF=bis(ethylenedithio)tetrathiofulvalene) This has resulted in efficient piezo-resistive organic molecular sensors. Conversely, solubility and other incompatibilities limit the direct application of the crystallite growth method to other substrates with arbitrary shape and composition. Here we report methods to circumvent these limitations. Specifically, we demonstrate the transfer of the active layer of a PC/(BEDT-TTF)₂I₃ bilayer film from the non-porous parent PC substrate to porous and humidity-dependent *Bombyx mori* silk target substrates. SEM, temperature dependent resistance, and electromechanical measurements show no significant damage to the transferred (BEDT-TTF)₂I₃ layer. The silk/(BEDT-TTF)₂I₃ bilayer films exhibit additional functions that can be used for humidity sensing, electric current-driven actuators, and strain detection. Of particular significance is the piezoresistive function of the porous silk bilayer structure that allows the investigation of multi-stage diffusion processes.

Introduction

Organic molecular conducting materials are well known for their high quality single crystalline form, and for wide range of physical properties including insulating, semiconducting, metallic, magnetic and superconducting phases.¹⁻⁹ Most often, these materials are formed as charge transfer salts in the form D₂M,

where D^{+1/2} is a planar organic donor, and M⁻¹ is an inorganic acceptor; as a result the donor (chains or layers) have unfilled bands and are metallic at room temperature.¹⁰⁻¹³ Until recently, the soft-organic and small-sized (~ 1 mm³) nature of single crystals and the dendritic bulk morphology of electrochemical growth by oxidation methods has prohibited any standard method of scale-up processing into thin films for device or sensor applications. A breakthrough¹⁴⁻¹⁶ came with the discovery that the oxidation reaction could proceed by mixing the donor component BEDT-TTF (bis(ethylenedithio)tetrathiofulvalene) in its neutral state into a polycarbonate (PC) thin film that then is exposed to an acceptor like iodine, expressed in a solvent vapor. This produced self-assembling polycrystalline layer composed of physically and electronically interconnected sub-micron crystallites on the top of the exposed surface of the PC film that respond reliably to bending strain,¹⁷ yielding a new class of flexible organic molecule-based sensors.^{18,19}

Unfortunately, the chemical growth method is compatible only with solvent soluble polymer substrates, prohibiting its direct use to cover substrates of interest with variable (sculpted) shapes and compositions. For example, it is very difficult to infuse the BEDT-TTF molecules into silk materials homogeneously prior to the oxidation due to either solvent incompatibilities or the tendencies of the BEDT-TTF molecules to crystallize in silk environments prior to the oxidation process (see Electronic Supplementary Information (ESI), Figure S1). The purpose of the present work is to show how the functional thin polycrystalline layers can be transferred from a non-porous PC substrate to a substrate that has both shape and humidity-dependent functions, setting the stage for future applications of molecular conductors. Here we demonstrate methods of transferring the active layer of highly piezoresistive PC/(BEDT-TTF)₂I₃ (pristine) bilayer films from the parent PC substrate to *Bombyx mori* silk film target substrates.

(BEDT-TTF)₂I₃ salt can be obtained in five different crystal phases, two of which are more common, α - and β -(BEDT-TTF)₂I₃, where the semimetal α -phase and superconducting β -phase are semiconducting and metallic as polycrystalline layers, respectively.¹⁵ The transferred (BEDT-TTF)₂I₃ layers (for both α - and β -phases) are robust, exhibiting similar surface and electrical properties to those of the pristine bilayers as confirmed by SEM, temperature dependent resistance, and electromechanical measurements. In comparison to the pristine bilayer films, the silk/(BEDT-TTF)₂I₃ bilayer films exhibit additional functions, allowing electronic monitoring of humidity and electrical current actuated functions (see ESI, Movie S1). A unique aspect of this novel silk bilayer structure is that the humidity dependent resistance provides new ways to address complex diffusion effects in porous substrates such as the *Bombyx mori* silk film. By correlating moisture-induced changes in the silk structure to the piezoresistive properties of the (BEDT-TTF)₂I₃ layer, a non-Fickian, multi-stage moisture absorption process in the silk layer is revealed. In addition to silk substrates, the layer transfer can also be directly applied to rubber, silica, glass, sculpted plastic products, paper, and substrates with various shapes and geometry.

Results and discussion

In the present work we have used PC/(BEDT-TTF)₂I₃ bilayer films with the α -(BEDT-TTF)₂I₃ salt for strain studies. By heat treatment of such bilayer films, the α -(BEDT-TTF)₂I₃ active layer can be transformed into a more thermodynamically stable β -(BEDT-TTF)₂I₃ active layer¹⁵ which we have used for humidity studies and electrical current actuator demonstrations. Both (referred to generically as (BEDT-TTF)₂I₃) are electrically conducting and piezoresistive at room temperature. To cover different substrates with (BEDT-TTF)₂I₃ active layers, we have developed two different procedures (Figure 1) to transfer the (BEDT-TTF)₂I₃ layers grown at the surface of a parent PC support to receiving substrates.

The first procedure, referred hereafter as the face-down layer transfer, where the active layer face of the pristine bilayer is oriented down toward the receiver substrate, is most suitable for covering various flat substrates (Figure 1a and 1c). The second procedure, namely the face-up layer transfer (active layer face oriented up and away from the receiver substrate), is more universal; it allows the covering of sculpted substrates (Figure 1b and 1d). In both cases, the transfers involve the separation of the (BEDT-TTF)₂I₃ layers from a parent PC substrate by dissolving the PC layer using a small amount of dichloromethane (DCM). Additional experimental details are given in the ESI (Figure S2-S8).

Face-Down Layer Transfer

Applicability of the face-down approach of covering substrates with molecular metals (see ESI, Figure S2 and S3) is considered in detail using examples of the (BEDT-TTF)₂I₃ layer transfers from a parent PC support to a receiver *Bombyx mori* silk film; a material considered as one of the ideal substrates for

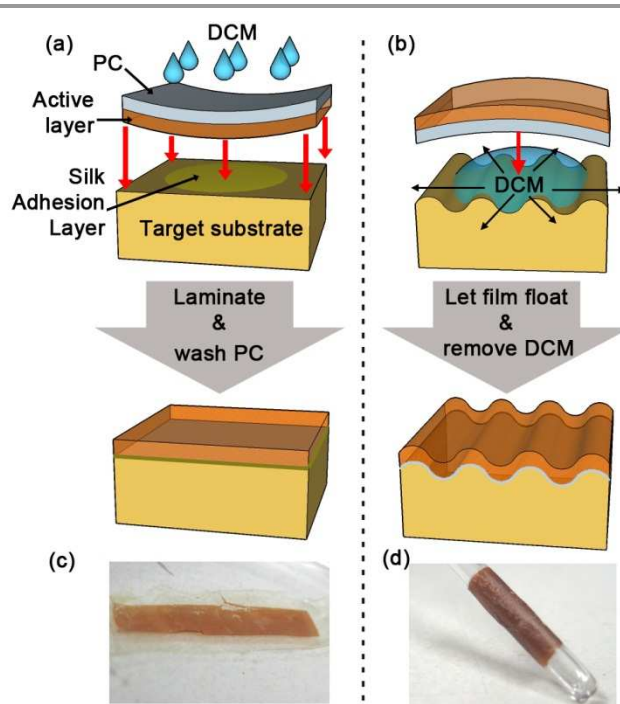


Figure 1. Layer transfer schematics. Overview of the (a) face-down and (b) face-up layer transfer methods. Photographs of the transferred strain sensing layer of α -(BEDT-TTF)₂I₃ molecular semimetal (c) to a silk film via face-down approach and (d) to a glass tube of \varnothing 3 mm via face-up approach.

implantable devices.^{20,21} The silk film is prepared via drop casting a \sim 8 % (wt/vol) solution of silk in water on a polystyrene dish. The silk solution is obtained by following the procedure reported in Ref. 22, which involves the fiber extraction from raw *Bombyx mori* cocoons (purchased from Aurora Silk) using a 0.02 M Na₂CO₃ solution, followed by fiber dissolving in a 9.3 M LiBr solution, purification by dialysis (Slide-A-Lyzer G-2 dialysis cassette, 3500 MWCO), and low temperature centrifugation.

To cover the silk film with a (BEDT-TTF)₂I₃ layer using the face-down layer transfer (see ESI, Figure S2 and S3), the silk film is first water-annealed²³ for 24 hours at 50 mbar to render it insoluble in water. Then, a thin *Bombyx mori* silk solution is deposited on the silk film to act as an adhesive layer. The BL films are laminated onto the wet silk surface by putting the top conductive (BEDT-TTF)₂I₃ layer of the BL film face down on the substrate. The conductive layer of the BL film can be pre-treated by argon plasma for 10 seconds to improve its homogenous adhesion to the receiver silk film. Lamination is completed by using a commercial smooth polytetrafluoroethylene-based plate. To remove the PC layer, we drop DCM over the film at an angle to allow the solvent containing dissolved PC to flow away. The complete removal of PC layer can be checked by either measuring the electrical resistance of the film or through direct observation under an optical microscope (see ESI, Figure S4).

Surface and Interface Structures

The face-down layer transfer allowed us for the first time to study the texture of the reverse side of the conductive α -(BEDT-TTF)₂I₃ layer formed at the interface with the PC film. Micro-scale

COMMUNICATION

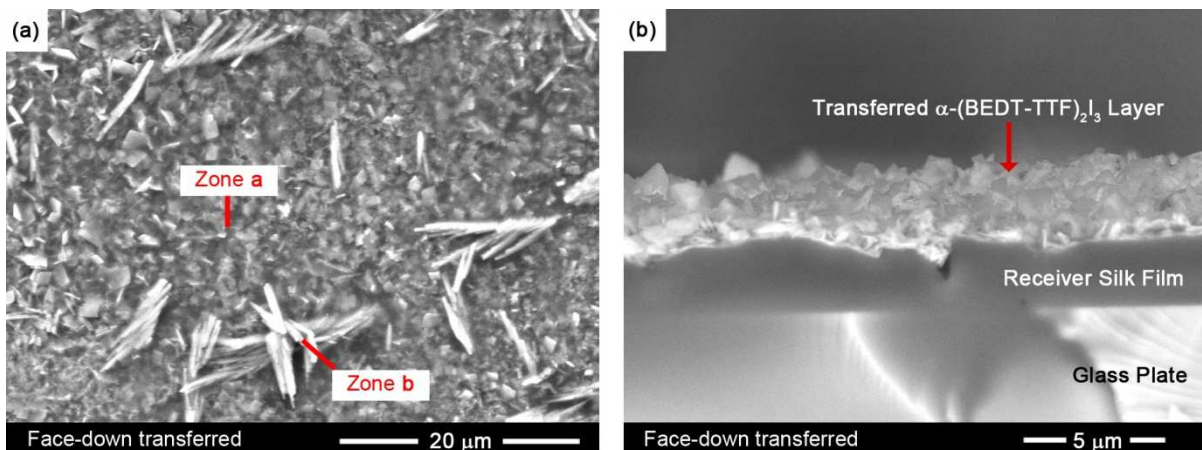


Figure 2. SEM images of face-down transferred α -(BEDT-TTF) $_2$ I $_3$ layers. (a) Surface and (b) cross-section profile of a silk/ α -(BEDT-TTF) $_2$ I $_3$ bilayer; the silk film was cast on a glass slide. The surface profile reveals the back side arrangement of the conductive α -(BEDT-TTF) $_2$ I $_3$ layer initially formed on the parent PC film. Zones a and b correspond to the reacted and un-reacted (BEDT-TTF) compound, respectively.

surface analysis was performed using a SEM (Quanta FEI 200 FEG-ESEM) with an EDAX spectrometer. As presented in Figure 2a, we observed a small number of crystallite aggregates (zone b) on the reverse side of the otherwise smooth conducting layer (zone a). Using EDAX analysis the contribution of elemental I and S atoms to the composition of zone a was found to be (18.2 ± 0.5) and (81.8 ± 0.5) atomic %, respectively.

Therefore, zone a has an average (BEDT-TTF) $_2$ I $_3$ composition that is in reasonable agreement with the expected stoichiometric formula α -(BEDT-TTF) $_2$ I $_3$. In contrast, zone b contains a very small amount of iodine: the contribution of I and S to their compositions was found to be (1.5 ± 0.5) and (98.5 ± 0.5) atomic %, respectively. Based on this observation, the minor crystallite aggregates of crystals have average (BEDT-TTF) $_2$ I $_3$ composition. This suggests that during the BL film preparation,¹³⁻¹⁵ un-reacted BEDT-TTF may crystallize on the back side of the conductive layer.

The cross section of the silk/ α -(BEDT-TTF) $_2$ I $_3$ bilayer was also studied by SEM. As evident from the Figure 2b, the transferred α -(BEDT-TTF) $_2$ I $_3$ -based layer has a good intimate contact with the receiver silk film similar to that of the pristine PC/ α -(BEDT-TTF) $_2$ I $_3$ bilayer films. Using the same film lamination principle, the face-down layer transfer may be used for covering various flat substrates including paper sheets; the paper sheets can be covered with combinations of α - and β -(BEDT-TTF) $_2$ I $_3$ as desired to form conductive sensing paper (see ESI, Figure S5 and S6).

Electronic Properties

In addition to the similar surface and interfacial structures, the silk/(BEDT-TTF) $_2$ I $_3$ and PC/(BEDT-TTF) $_2$ I $_3$ bilayer films also

exhibit similar temperature dependent resistance and electromechanical behavior. The α - and β -(BEDT-TTF) $_2$ I $_3$ layers before and after layer transfer were examined by four probe direct current (DC) resistance measurements with carbon paste electrodes using a Keithley 6221 current source and a Keithley 2182A nanovoltmeter. As evident in Figure 3a and 3b, both original (PC) and transferred (silk) α - and β -(BEDT-TTF) $_2$ I $_3$ layers demonstrate basically the same temperature-dependent electronic transport properties. It should be noted that in comparison with the original PC/ α -(BEDT-TTF) $_2$ I $_3$ layer, the silk/ α -(BEDT-TTF) $_2$ I $_3$ transferred layer exhibits a slightly broader semimetal-to-insulator transition.

The data presented in Figure 3c show that the electrical resistance of the transferred α -(BEDT-TTF) $_2$ I $_3$ layer on a silk film exhibits a reversible linear response to relative strain (ϵ). The value of strain sensitivity (gauge factor) is 9, in a good agreement with previously reported values.⁹ The gauge factor is defined as the ratio between the relative resistance change ($\Delta R/R_0$) and the relative strain value ($\epsilon = \Delta L/L_0$), where $\Delta R = R_e - R_0$, $\Delta L = L - L_0$, L is uniaxial elongation, and L_0 is the gauge length.

Humidity Dependence

In contrast to the pristine PC/(BEDT-TTF) $_2$ I $_3$ bilayer film, the silk/(BEDT-TTF) $_2$ I $_3$ BL film exhibits electric current-actuated functions (see ESI, movie S1) and a humidity dependent resistance. Due to the softness of the piezoresistive molecular conductor crystals and their intimate contact with the silk

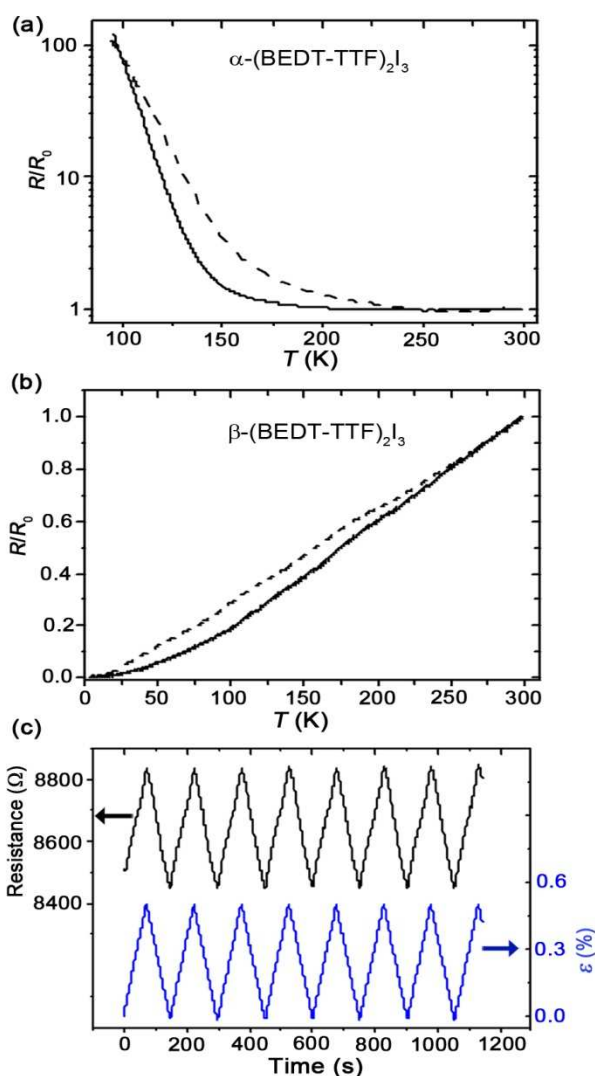


Figure 3. Electronic and electromechanical properties of the face-down transferred sensing layer. Temperature dependence of the normalized resistance of the original (PC- solid line) and transferred (silk- dash line) layers of (a) α - and (b) β -(BEDT-TTF) $_2$ I $_3$. (c) Resistance changes of the transferred silk/ α -(BEDT-TTF) $_2$ I $_3$ layer with time upon an application of 7 cycles of monoaxial elongations performed at a strain rate of 0.3 $\mu\text{m/s}$. The layer was transferred on a silk film using the face-down transfer approach. Resistance and elongation data were measured every 0.5 s during the multi-cyclic deformations on a film with a length of 1.2 cm.

substrate, the resistance is well-coupled to the swelling/de-swelling of the silk substrate under varying humidity conditions. This also allows us to study the water absorption mechanism of *Bombyx mori* silk via electrical transport measurements. The humidity dependent resistance measurement was performed inside an environmental chamber at 23 $^{\circ}\text{C}$ in a 4-contact configuration using a lock-in amplifier (see ESI, Figure S9). A separate humidity sensor (HIH-5030) was mounted in close proximity to the BL film.

As evident in Figure 4a, the resistance of the BL film reversibly tracks the relative humidity (RH) changes in the surrounding environment. A delay in the humidity response is observed (Figure 4b) even though the RH is varied slowly

($\sim 0.025\%$ / s), indicating a diffusion-limited moisture absorption process of the *Bombyx mori* silk film. The humidity response can be modelled by considering the general solution to a resistor-capacitor (RC) charging circuit where the charging voltage varies with time. In this model (Equation 1), for any specific time t , the supply voltage V_s is analogous to RH, the capacitor voltage V_c is analogous to the moisture uptake (and swelling of the silk that produces a change in the film resistance), V_r is the initial capacitor voltage (analogous to initial moisture content) at the start of the charging process, and τ is the diffusion relaxation time constant analogous to RC. In equilibrium and/or for $\tau \rightarrow 0$, the moisture uptake ($\sim V_c$) is directly proportional to the RH ($\sim V_s$). Since in the bilayer film we measure the piezoresistance which is analogous to the capacitor voltage, we may recast Equation 1 as Equation 2a under the assumption in Equation 2b that RH drives the time dependence.

$$V_c(t) = V_s(t)(1 - e^{-t/\tau}) + V_r e^{-t/\tau} \quad (1)$$

\Downarrow

$$R(t) - R_0 = R_s(t)(1 - e^{-t/\tau}) + R_r e^{-t/\tau} \quad (2a)$$

$$R_s(t) = A * RH(t) \quad (2b)$$

Explicitly, the analogy is that $R(t)$ is the resistance of the BL film at any given time, R_0 is the resistance of a completely dried film, $R_s(t)$ is the resistance of saturated film at a given RH value, R_r is the resistance due to trapped residual moisture content at the beginning of absorption process, and τ is the time constant of the humidity response. In Figure 4b, R_0 , R_r , proportionality constant A , and τ are determined to be 6.8 k Ω , 1 k Ω , 33.4 $\Omega/\text{RH}\%$, and 645 s.

Although this model fits well to the data in Figure 4b, the model breaks down at faster sweep rates. For the measurement obtained at a higher RH rate (0.125 % / s), it is not possible to fit the data perfectly using the model (see ESI, Figure S5). This leads us to believe that the moisture absorption process is more complex than that described by the simple RC circuit model.

To study the moisture absorption process in more detail, a step function exposure experiment was performed. The BL film was first dried overnight at 23 $^{\circ}\text{C}$ and 30 % RH, after which the film was suddenly exposed to a constant, saturated 73 % RH environment. In Figure 4c, the time dependent resistance after the sudden exposure is presented, showing features that deviate from the Fickian moisture absorption process.^{24,25} First, there is no clear saturation level²⁶ that is typically observed in a Fickian process, at least within the given time scale. Instead, the resistance continues to slowly increase at larger times. Second, the normalized resistance ($\Delta R(t)/\Delta R_{\text{max}}$) varies with time (t) according to the following function, $\Delta R(t)/\Delta R_{\text{max}} \sim t^n$, where $\Delta R(t) = R(t) - R(\text{at } 30\% \text{ RH})$, $\Delta R_{\text{max}} = R(\text{at } 73\% \text{ RH}) - R(\text{at } 30\% \text{ RH})$, and $n = 0.83$ (Figure 4c). In a Fickian process, $n =$

COMMUNICATION

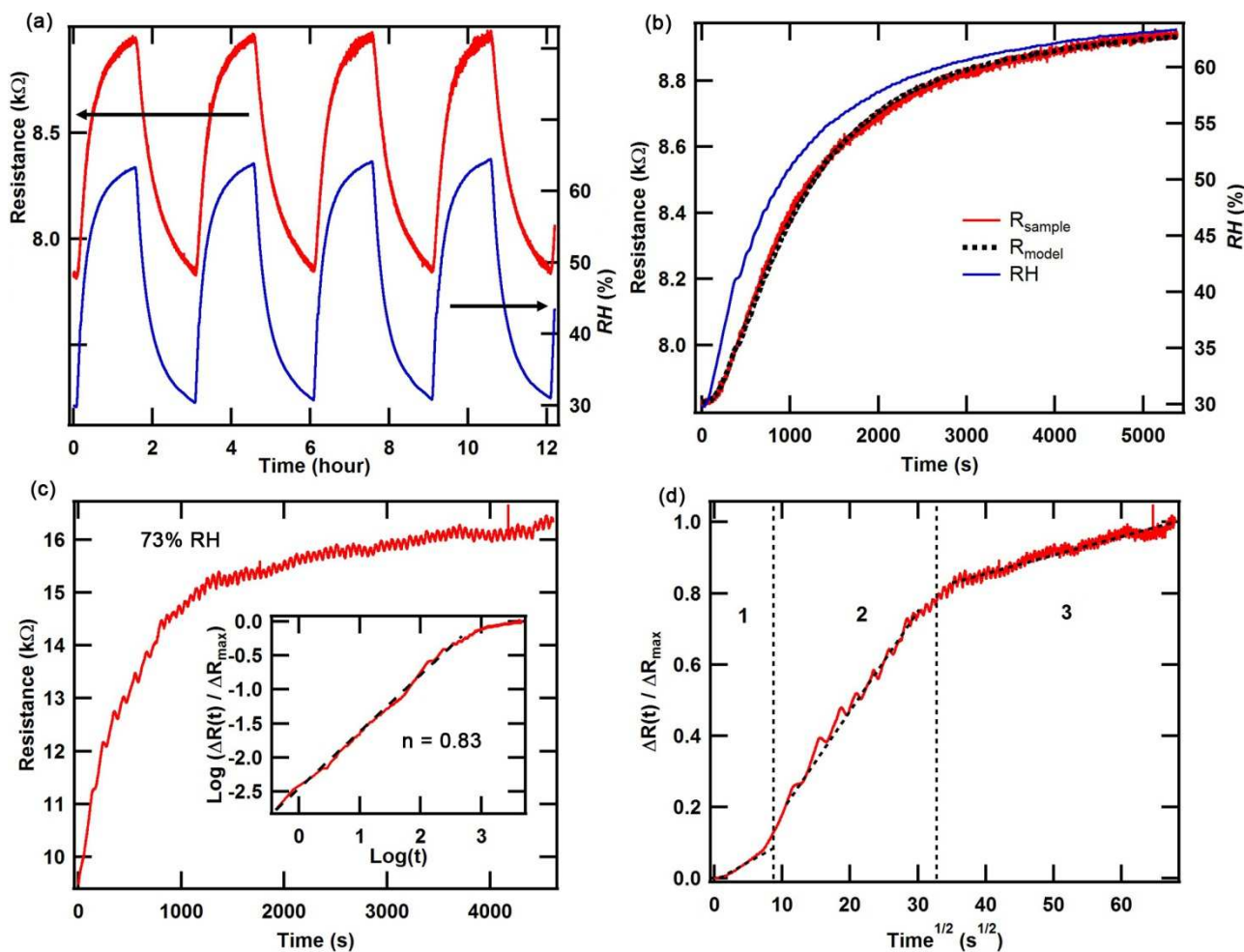


Figure 4. Humidity monitoring via electrical response of *Bombyx mori* silk/ β -(BEDT-TTF) $_2$ I $_3$. (a) Cyclic RH monitoring. Maximum RH sweep rate ~ 0.025 % / s. (b) Fit to the data using a capacitor charging model. (c) Time dependent resistance of a flash humidity exposed BL film at 23 °C and 73 % RH. Inset: log-log plot of the normalized resistance vs time. The value of power factor, n , is extracted from the slope indicated by the dotted line. (d) Fick $t^{1/2}$ plot of the time dependent resistance during the step-function humidity exposure.

0.5 at the initial stage of absorption.^{24,27} These features are similar to the cases reported in the literature²⁶ involving a dual-stage moisture diffusion process,^{25, 26} where the first and second stages are attributed to void-filling and hydrogen bonding processes.²⁸ As shown in Figure 4d, there are 3 distinct stages of diffusion. The first stage can be attributed to film expansion mainly due to the filling of voids in the silk film. As the absorption transitions to the second stage, moisture continues to fill the voids but also penetrates and forms hydrogen bonds with the silk protein, swelling the protein internally. Finally in the third stage, all the voids have been filled but internal swelling continues to progress deeper into the silk structures. This result highlights the

complex mechanisms of water transport processes in *Bombyx mori* silk.

Face-Up Layer Transfer

For applications requiring the covering of sculpted substrates (see ESI, Figure S7 and S8), the face-up approach is used, where the top conductive (BEDT-TTF) $_2$ I $_3$ layer of the bilayer films faces up on the substrate. Whereas the face-down layer transfer relies on the effectiveness of mechanical lamination, the face-up layer transfer is based on the thinning and swelling of the underlying PC resulting in an active layer that naturally conforms to the shape of the target substrate. In this case, unlike the face-

COMMUNICATION

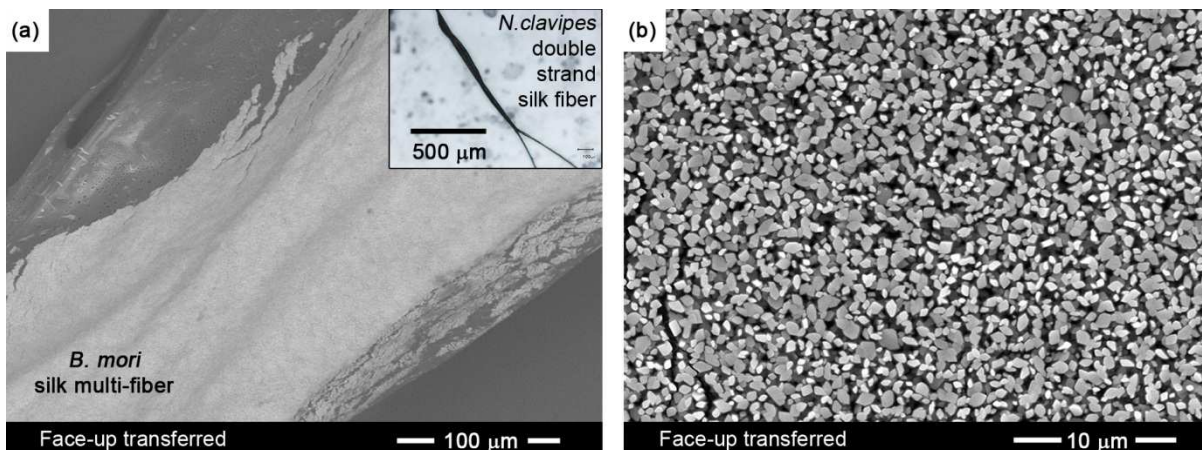


Figure 5. SEM images of the face-up transferred α -(BEDT-TTF) $_2$ I $_3$ layer. (a) Low and high (b) magnification images of the face-up transferred layer on a *Bombyx mori* silk multi-fiber. SEM images were acquired by scanning electron microscope (SEM) HITACHI S-3000N on a Hitachi S-570 system operating at 10 kV. Inset in (a) corresponds to a photograph of covered *Nephila clavipes* double-strand dragline silk fibers.

down layer transfer (Figure 2) where the PC is completely removed, the face-up layer transfer (Figure 5) requires a thin PC-based under-layer to maintain the integrity of the transferred conducting (BEDT-TTF) $_2$ I $_3$ layer and for adhesion to the substrate. The general approach of the face-up layer transfer (Figure 1b) is outlined in the following: (i) a pool of DCM is deposited on a target substrate; (ii) the BL film is placed on the surface of the pool with the PC support facing down and the conducting side of the BL film facing up; (iii) after the BL film floats and softens for some seconds, the DCM-based pool is removed using an absorbent; (iv) the conductive sensing (BEDT-TTF) $_2$ I $_3$ layer then conforms to the surface geometry of the target substrate (Figure 5a). The SEM image of highest magnification (Figure 5b) demonstrates that minimal cracking occurs after the conductive layer is transferred.

Conclusions

In this work, we highlight the robustness of the BL film grown by the one-stage oxidative/annealing approach and when combined with the layer transfer processes we have developed, the BL film is demonstrated to be highly versatile. To the best of our knowledge this work gives the first demonstration of the capability to cover substrates, which are different in composition and geometric form, with flexible all-organic electrical strain sensing layers of molecular conductors (see Supporting Information, Movie S2). The layer transfer processes do not significantly change the electronic transport and electromechanical properties of the strain sensing polycrystalline layers of the (BEDT-TTF) $_2$ I $_3$ conductors that are initially formed on parent PC substrates. In addition to various potential device

applications, such as for humidity sensors and electrical current driven actuators, the sensing layer can also be used to study water diffusion processes. Our results should open the door to novel applications of organic molecular metals in sensing and other related technologies, and for thin film porous substrate materials, new ways to study complex diffusion processes where there is a coupling between the material volume and the diffusion species.

Acknowledgements

Work by E.S. is supported by NSF-DMR 1005293 and 1309146. A portion of this work was performed at the National High Magnetic Field Laboratory, which is supported by NSF Cooperative Agreement No. DMR-0654118, by the State of Florida, and by the DOE. This work was supported in part by the Spanish Dirección General de Investigación (DGI) (project POMAs, CTQ2010-19501/BQU), the Generalitat de Catalunya (2009SGR00516), E.L. thanks CIBER-BBN, an initiative funded by the VI National R&D&i Plan 2008-2011, Iniciativa Ingenio 2010, Consolider Program, CIBER Actions and financed by the Instituto de Salud Carlos III with assistance from the European Regional Development Fund and V. L. acknowledges a grant FI-DGR from the Generalitat de Catalunya.

Notes and references

^a Department of Physics and National High Magnetic Field Laboratory Florida State University 1800 East Paul Dirac Drive, Tallahassee, Florida 32310 (United States).

^b Institut de Ciència de Materials de Barcelona (ICMAB-CSIC) Campus UAB, Bellaterra, 08193, (Spain).

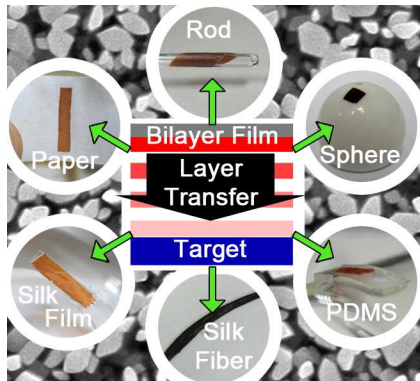
^c CIBER de Bioingeniería, Biomateriales y Nanomedicina (CIBER-BBN), Campus UAB, Bellaterra, 08193, (Spain).

^d Institució Catalana de Recerca i Estudis Avançats (ICREA), ICMAB-CSIC, Campus UAB, Bellaterra, 08193, (Spain). E-mail: esteven@magnet.fsu.edu; laukhina@icmab.es.

Electronic Supplementary Information (ESI) available: [images of formation of BEDT-TTF crystals on *Bombyx mori* silk, photos of different preparation stage for both face-down and face-up are shown; as well as electronic and electromechanical properties of (BEDT-TTF)₂13-covered paper and set-up of humidity experiments and obtained data are presented, two movies demonstrate Silk/□-(BEDT-TTF)₂13 electric current-driven actuator and deformation sensitivity text using flexible pipette]. See DOI: 10.1039/c000000x/

- 1 T. Ishiguro, K. Yamaji, G. Saito, *Organic Superconductors*, Second Ed., Springer, Heidelberg 1998.
- 2 H. Akamatu, H. Inokuchi and Y. Matsunaga, *Nature* 1954, **173**, 168.
- 3 J. Ferraris, D. O. Cowan, V. Walatka and J. H. Perlstein, *J. Am. Chem. Soc.* 1973, **95**, 948.
- 4 S. S. P. Parkin, E. M. Engler, R. R. Schumaker, R. Lagier, V. Y. Lee, J. C. Scott and R. L. Greene, *Phys. Rev. Lett.*, 1983, 270.
- 5 P. M. Chaikin, J. F. Kwak, T. E. Jones, A. F. Garito and A. J. Heeger, *Phys. Rev. Lett.* 1973, **31**, 601.
- 6 E. B. Yagubskii, I. F. Schegolev, V. N. Laukhin, R. P. Shibaeva, E. E. Kostyuchenko, A. G. Khomenko, Y. V. Sushko and A. V. Zvarykina, *Pis'ma v ZhETF* 1984, **40**, 387.
- 7 D. Jerome, *Chem. Rev.* 2004, **104**, 5565.
- 8 X. Yan, M. J. Naughton, R. V. Chamberlin, S. Y. Hsu, L. Y. Chiang, J. S. Brooks and P. M. Chaikin, *Phys. Rev. B* 1987, **36**, 1799.
- 9 M. Tokumoto, H. Anzai, H. Bando, G. Saito, N. Kinoshita and K. Kajimura, T. Ishiguro, *J. Phys. Soc. Jpn.* 1985, **54**, 869.
- 10 K. Bechgaard, C. S. Jacobsen, K. Mortensen, H. J. Pedersen and N. Thorup, *Solid State Commun.* 1980, **33**, 1119.
- 11 G. Saito, *Organic Molecular Solids*, CRC, Boca Raton, FL, USA 1997, Ch. 10.
- 12 R. P. Shibaeva and E. B. Yagubskii, *Chem. Rev.* 2004, **104**, 5347.
- 13 G. Saito and Y. Yoshida, *Bull. Chem. Soc. Jpn.* 2007, **80**, 1.
- 14 J. K. Jeszka and A. Tracz, *Polym. Adv. Technol.* 1992, **3**, 139;
- 15 E. Laukhina, C. Rovira and J. Ulanski, *Synth. Met.* 2001, **21**, 1407;
- 16 T. Haneda, A. Tracz, G. Saito and H. Yamochi, *J. Mater. Chem.* 2011, **21**, 1621.
- 17 E. Laukhina, R. Pfattner, L. R. Ferreras, S. Galli, M. Mas-Torrent, N. Masciocchi, V. Laukhin, C. Rovira and J. Veciana, *Adv. Mater.* 2010, **22**, 977.
- 18 V. Laukhin, I. Sanchez, A. Moya, E. Laukhina, R. Martin, F. Ussa, C. Rovira, A. Guimera, R. Villa, J. Aguilo, J.-C. Pastor and J. Veciana, *Sens. Actuators A* 2011, **170**, 36.
- 19 L. R. Ferreras, R. Pfattner, M. Mas-Torrent, E. Laukhina, L. Lopez, V. Laukhin, C. Rovira and J. Veciana, *Mater. Chem.* 2011, **21**, 637.
- 20 D.-H. Kim, J. Viventi, J. J. Amsden, J. Xiao, L. Vigeland, Y.-S. Kim, J. A. Blanco, B. Panilaitis, E. S. Frechette, D. Contreras, D. L. Kaplan, F. G. Omenetto, Y. Huang, K.-C. Hwang, M. R. Zakin, B. Litt and J. A. Rogers, *Nature Mater.* 2010, **9**, 511.
- 21 S.-W. Hwang, H. tao, D.-H. Kim, H. Cheng, J.-K. Song, E. Rill, M. A. Brenckle, B. Panilaitis, S. M. Won, Y.-S. Kim, Y. M. Song, K. J. Yu, A. Ameen, R. Li, Y. Su, M. Yang, D. L. Kaplan, M. R. Zakin, M. J. Slepian, Y. Huang, F. G. Omenetto and J. A. Rogers, *Science* 2012, **337**, 1640.
- 22 D. N. Rockwood, R. C. Preda, T. Yucel, X. Wang, M. L. Lovett and D. L. Kaplan, *Nat. Protoc.* 2011, **6**, 1612.
- 23 Q. Lu, X. Hu, X. Wang, J. A. Kluge, S. Lu, P. Cebe and D. L. Kaplan, *Acta Biomater.* 2010, **6**, 1380.
- 24 J. T. Alfrey, E. F. Gurnee and W. G. Lloyd, *J. Poly. Sci. C* 1966, **12**, 249.
- 25 Y. J. Weitsman, *Composites Part A* 2006, **37**, 617.
- 26 M. H. Shirangi, X. J. Fan and B. Michel, in *Micro- and Opto-Electronic Materials, Structures, and Systems*, (Eds: X. J. Fan, E. Suhir), Springer US, 2010, 29.
- 27 Z. Ahmad, M. P. Ansell and D. Smedley, *IOP Conf. Series: Materials Science and Engineering* 2011, **17**, 012011.
- 28 H. G. Carter and K. G. Kibler, *J. Comp. Mater.* 1978, **12**, 118.

Table of Content



A polycrystalline layer of $(\text{BEDT-TTF})_2\text{I}_3$ -based molecular conductor is transferred from a polycarbonate template to silk and other substrates for sensing and actuation applications.